

TOWARD IMPROVED HEAT DISSIPATION OF THE TURBULENT REGIME OVER BACKWARD-FACING STEP FOR THE Al_2O_3 -WATER NANOFLUIDS: An Experimental Approach

by

**Syed Muzamil AHMED^{a*}, Salim Newaz KAZI^{a*}, Ghulamullah KHAN^d,
Mohd Nashrul Mohd ZUBIR^a, Mahidzal DAHARI^b, Suriani IBRAHIM^a,
Mohammad Sofian abu TALIP^a, Pervaiz AHMAD^c, and
Zaira Zaman CHOWDHURY^e**

^aDepartment of Mechanical Engineering, Faculty of Engineering, University of Malaya, Kuala Lumpur, Malaysia

^bDepartment of Electrical Engineering, Faculty of Engineering, University of Malaya, Kuala Lumpur, Malaysia

^cDepartment of Physics, University of Azad Jammu and Kashmir, Muzaffarabad, Pakistan

^dDepartment of Chemical Engineering, Balochistan University of Information Technology, Engineering and Management Sciences, Quetta, Pakistan

^eNanotechnology and Catalysis Research Centre (NANOCAT), University of Malaya, Kuala Lumpur, Malaysia

Original scientific paper
<https://doi.org/10.2298/TSCI170606236A>

Experimental study of nanofluid flow and heat transfer to fully developed turbulent forced convection flow in a uniformly heated tubular horizontal backward-facing step has reported in the present study. To study the forced convective heat transfer coefficient in the turbulent regime, an experimental study is performed at a different weight concentration of Al_2O_3 nanoparticles. The experiment had conducted for water and Al_2O_3 -water nanofluid for the concentration range of 0 to 0.1 wt.% and Reynolds number of 4000 to 16000. The average heat transfer coefficient ratio increases significantly as Reynolds number increasing, increased from 9.6% at Reynolds number of 4000 to 26.3% at Reynolds number of 16000 at the constant weight concentration of 0.1%. The Al_2O_3 -water nanofluid exhibited excellent thermal performance in the tube with a backward-facing step in comparison to distilled water. However, the pressure losses increased with the increase of the Reynolds number and/or the weight concentrations, but the enhancement rates were insignificant.

Key words: backward-facing step, heat transfer, nanofluids, re-circulation flow

Introduction

Separation, re-circulation regions, and consequent reattachment due to sudden expansion in flow geometry, such as a backward-facing step (BFS), play an important role in fluid mechanics and many engineering applications, where heat transfer occurs. This sudden expansion present in heating or cooling applications such as high performance heat exchangers, chemical processes, combustion chambers, cooling of nuclear reactors, cooling turbines blades, cooling electronic equipment, and wide-angle diffusers, *etc.* In many circumstances, sudden expansion is undesirable and could be the source of enhanced pressure drop along with energy losses that require additional power supply.

Corresponding author, e-mail: syed.ma@hotmail.com

However, in many instances sudden expansions are encouraged, these lead to the enhanced heat and mass transfer rates due to higher mixing in separation and reattachment flow regions [1]. Because of this reality, the problem of laminar and turbulent flows over backward-facing and forward-facing steps test loop in natural, mixed and forced convection have been extensively investigated, both numerically and experimentally [2].

Conventional heat transfer fluids such as water, oil, and ethylene glycol have characteristically low thermal conductivity than metal oxides and metals. Consequently, heat transfer characteristics of fluids are expected to be better than traditional heat transfer fluids upon suspending solid particles [3]. But fluids with suspended particles of a millimeter or micrometer size in the practical application used as a coolants source have some problems, such as corrosion, erosion, instability of particles, clogging of flow channels, and additional pressure drop [4-6]. In contrast, many researchers have reported that the convective heat transfer coefficient and the effective thermal conductivity of the base fluid can be enhanced via dispersing solid nanoparticles of a high thermal conductivity in conventional base fluids [7-11]. Solid particles can be metallic such as Al_2O_3 , SiO_2 , CuO , Cu , ZnO and TiO_2 , and nonmetallic *e. g.* carbon and graphene nanoparticles, *etc.* [12-14]. Many researchers investigated flow separation in the past decades. The pioneer researchers Boelter, *et al.*, [15], Ede, *et al.*, [16], Seban [17], Abbott and Kline [18], Filetti and Kays [19], Goldstein, *et al.*, [20] established theoretical and experimental methods of studying separation flow that take place due to changes in the cross-section of the passage. Abu-Nada [21] as a pioneer researcher reported laminar forced convective heat transfer coefficient over a duct with a sudden expansion in the presence of different nanofluids loaded with Al_2O_3 , TiO_2 , Cu , CuO , and Ag . He numerically investigated the effects of volume fractions between 0.05 and 0.2 and Reynolds numbers in the range of 200-600. He assumed 2-D laminar flow situation solving the backward-step flow problem numerically. An investigation of findings indicates that the Nusselt number has increased with the Reynolds number and volume fraction. Al-Aswadi, *et al.*, [22] have numerically investigated the laminar forced convective flow over a 2-D horizontal BFS in a duct by using finite volume method in the presence of different nanofluids. They have reported that the re-attachment length and recirculation size show enhancement with the increase of the Reynolds number. They concluded low dense nanoparticles such as SiO_2 exhibited the highest velocity than those with high dense nanoparticles such as Au . The effects of nanofluid on a mixed convective heat transfer over 2-D microscale BFS in the range of laminar flow are investigated numerically by Kherbeet, *et al.* [23]. They have used four types of nanoparticles; CuO , Al_2O_3 , ZnO , and SiO_2 , with a volume fraction range of 1-4%. Their results have revealed that SiO_2 nanofluid shows the highest Nusselt number among all the used nanofluids. It has also reported by them that with the increase of volume fraction of nanoparticles in the base fluid, the Nusselt number increases.

Recently, combined convection flows are investigated numerically over a 2-D forward-facing step with a blockage using different types of nanofluids (SiO_2 , Al_2O_3 , ZnO , and CuO), different diameters (25-80 nm) of nanoparticles and different volume fractions (1-4%), by Kherbeet, *et al.*, [24]. Additionally, effects of different shapes of blockage (square, circular, and triangular) in a test section were investigated. The aforementioned study has shown that the highest Nusselt number has achieved in the circular blockage followed by square blockage and triangular blockage. They have also reported that the nanofluids with SiO_2 nanoparticles have the highest Nusselt number. Conversely, the Nusselt number increases with the increase of volume fraction and Reynolds number and decreases as the nanoparticles diameter increases. The mixed convective flow over 3-D horizontal micro-scale BFS was investigated numerically by Kherbeet, *et al.*, [25]. In this study, ethylene glycol (EG)-based SiO_2 nanofluid with a nanoparticle diameter

of 25 nm and volume fraction of 0.04% has been used. They have reported that with the increase of the step height the Nusselt number and skin friction coefficient increases. Their findings also have shown that the amount of pressure drop and Reynolds number decrease with an increase in the step height. More recently, Kherbeet, *et al.*, [26] experimentally investigated heat transfer characteristics of laminar nanofluid flow over the micro-scale forward-facing step and BFS. In their experimental investigation, the Reynolds number range of 280-480, the weight concentration of 1% and 0.5% with the SiO₂ diameter of 30 nm as an additive have used.

From the literature review, it is obvious that the experimental study of nanofluid flow and heat transfer over BFS in the turbulent flow regime seems have not taken under consideration. The aim of the present study is to investigate experimentally turbulent forced convective flow and heat transfer of Al₂O₃-water based nanofluid on a BFS with tubular geometry at constant heat flux. The deionized water has considered as a base fluid with Al₂O₃ nanoparticles suspended in the base fluid via sonication. The effects of the concentration of nanoparticles in the range of 0.0 to 0.1 weight percentages and Reynolds number in the range of 4000 to 16000 on heat transfer coefficient have been investigated. In addition, the effects of concentrations of nanoparticles and Reynolds number on pressure drop have also taken into consideration.

Experimental set-up

Experimental apparatus

The schematic of test rig applied in this study is shown in fig. 1. The flow loop consists of stainless steel piping, a jacketed tank connected with a chiller for cooling and heating of the stock solution up to the desired bulk temperature, a variable speed pump, a magnetic flow meter, differential pressure transducer, heated test section and recycles piping setup. Working fluids are pumped by a Cole Parmer TM magnetic drive pump from a 20 L capacity stainless steel jacketed tank and the fluid-flow rate being controlled by a Hoffman MullerTM inverter. An N-FLO-25 Electromagnetic flow meter and a FoxboroTM differential pressure transmitter, respectively, measured the flow rate and the pressure drop. The test section is a stainless-steel pipe of 800 mm length, 25.4 mm internal diameter with the separation ratio 2.

The outside wall of test section has insulated with a thick glass wool to minimize the amount of heat loss. The test section was heated by using two programmable DC power supply units (Agilent Technologies N8731A) with outputs of 8 V and output current of 400 A. Sixteen K type (Omega) thermocouples were mounted on the test section using high temperature epoxy glue on the outer surface of upstream of the test section. The positions of thermocouples are schematically presented in fig. 2. Besides, two RTD (PT - 100) sensors (Omega) were installed to obtain bulk temperature at the inlet and outlet of the test section. All the thermocouples including RTD were calibrated by Ametek temperature calibrator (AMETEK Test & Calibration Instruments, Denmark). The thermocouples and RTD were connected to the SCADA system for the continuous monitoring and recording of the temperature data by a WINCC software in a computer.

Preparation of nanofluids

Aluminum oxide powder (Al₂O₃ nanopowder with particle size ~50 nm), acquired from sigma Aldrich, and distilled water (Di-water) were used to prepare the Al₂O₃. Nanopowder of the desired amount was dispersed in Di-water by a probe sonicator for 30 minutes to have a homogeneous suspension. Four concentrations (0.025, 0.05, 0.075 and 0.1 wt.%) of Al₂O₃ were considered in this experimental study.

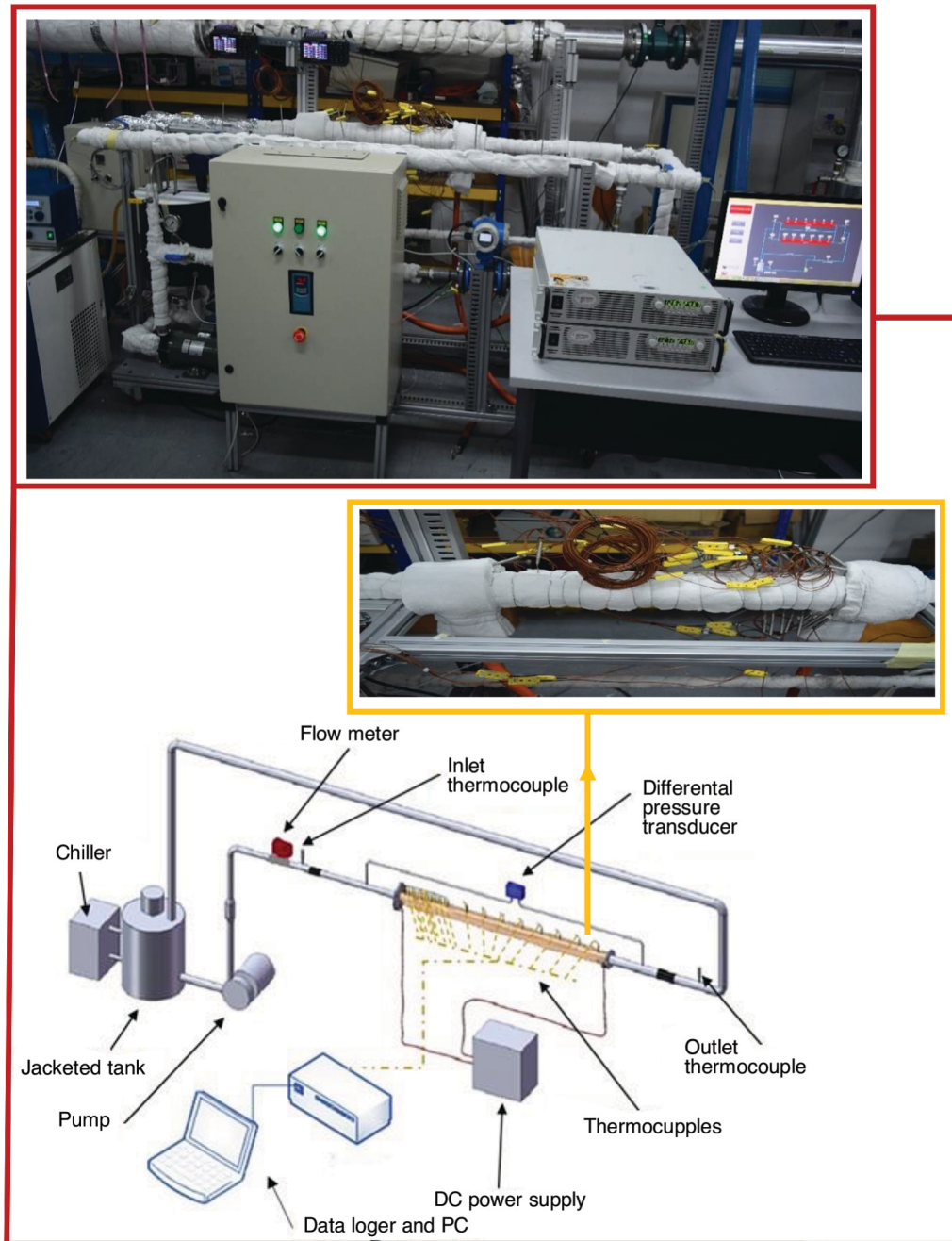


Figure 1. Schematic diagram of the experimental set-up

Experimental data reduction

The power supply and heat flux added to the downstream channel wall could be obtained from eqs. (1) and (3):

$$\Phi = VI \quad (1)$$

$$Q = \dot{m}C_p (T_{out} - T_{in}) \quad (2)$$

$$\dot{q} = \frac{Q}{A_w} \quad (3)$$

The local heat transfer coefficient, h_x , temperature of the bulk fluid, T_{bx} , and temperature of the wall, T_{wx} , have been obtained:

$$h_x = \frac{\dot{q}}{(T_{wx} - T_{bx})} \quad (4)$$

$$T_{bx} = T_{in} + \frac{L_x Q}{\dot{m}C_p} \quad (5)$$

$$T_w = T_{TC} - \dot{q}/(\lambda/x) \quad (6)$$

where T_{TC} is a surface temperature measured via a thermocouple and η is the percentage of heat transfer enhancement, which can be calculated from eq. (7). This parameter helps to well analyze the rate of enhancement in heat transfer after loading Al_2O_3 :

$$\eta = \frac{\bar{h}_{c,nf} - \bar{h}_{c,bf}}{\bar{h}_{c,bf}} 100 \quad (7)$$

where $\bar{h}_{c,nf}$, $\bar{h}_{c,bf}$ are the average heat transfer coefficient of nanofluid and the average heat transfer coefficient of base fluid, respectively.

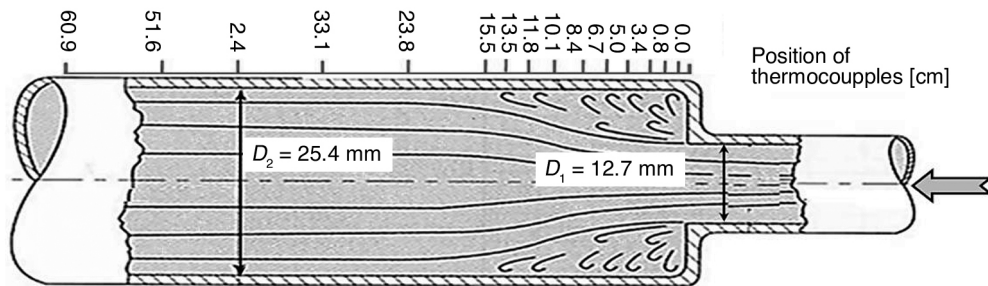


Figure 2. Schematic view of the test section

Using nanofluids in different heat exchangers increases both pressure drop and heat transfer coefficient [27, 28]. To evaluate the effectiveness of the nanofluid being used in the present study, performance index (PI) was selected as a suitable parameter and PI could be calculated from equation (8).

$$PI = \frac{\bar{h}_{c,nf} / \bar{h}_{c,bf}}{\Delta P_{nf} / \Delta P_{bf}} = \frac{R_h}{R_{\Delta P}} \quad (8)$$

where R_h is the ratio of the heat transfer of nanofluids to the base-fluid and $R_{\Delta P}$ is the ratio of the pressure drop of the nanofluids to the base fluid.

Results and discussion

For the first time, experimental investigation of heat transfer over a BFS using Al_2O_3 -water nanofluids is presented for the turbulent flow regime. Heat transfer over a BFS is investigated experimentally in the present study for different Reynolds numbers and weight concentrations of Al_2O_3 -water nanofluids.

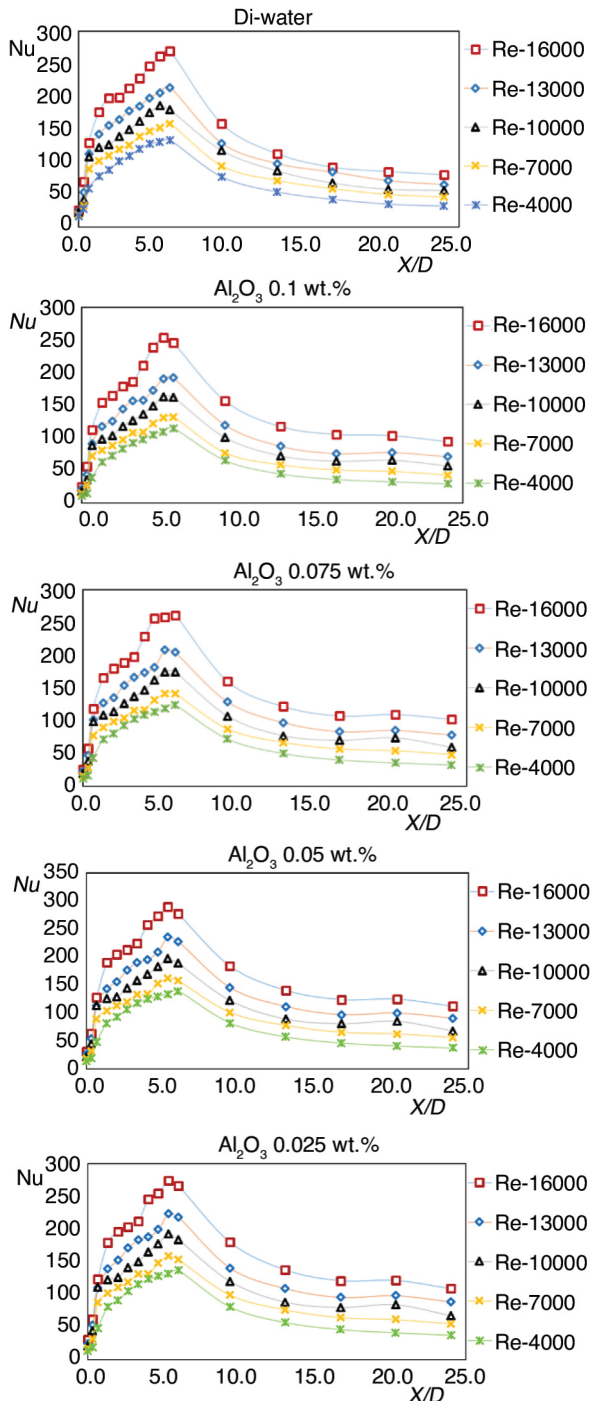


Figure 3. Experimental Nusselt number of Di-water and Al_2O_3 -water nanofluids at different weight concentrations of 0.025 wt.%, 0.05 wt.%, 0.075 wt.%, and 0.1 wt.% for different Reynolds numbers.

The effect of concentration of Al_2O_3 -water nanofluids on the Nusselt number at a range of Reynolds number 4000-16000 has been studied and the results present in fig. 3.

Distribution of the measured local Nusselt number (Nu_x) in the range of Reynolds number 4000-16000 for different weight concentrations (0.025, 0.05, 0.075 and 0.1 wt.%) of nanoparticles have compared with the Di-water data in fig. 3. The local Nusselt number peaked at the X/D range of 4 to 6 before starting to decrease gradually. The results in fig. 3 revealed that the prepared Al_2O_3 -water based nanofluids have higher Nu_x than that of pure water. Furthermore, an increase in the concentration of Al_2O_3 nanoparticles led to an enhancement in Nu_x . The region where the Nu_x values are increasing up to the maximum peak is the re-circulation zone and the zone where the Nu_x have peaked is the reattachment zone and consequently, the decrease of Nu_x after the maximum peak up to almost straight line is the zone where fluids become fully-developed.

For an appropriate evaluation of heat transfer, the average heat transfer coefficient of Al_2O_3 -water nanofluid was compared with water, h_c data at different weight concentrations (0.025, 0.05, 0.075 and 0.1 wt.%) over a range of Reynolds number, as shown in fig. 4(a). The average heat transfer coefficient increases with the increase of weight concentrations and Reynolds number. Contrary to the heat transfer to fiber suspensions, where h_c increases with the decrease of fiber concentration [29]. At the weight concentration of 0.1 wt.% and Reynolds number 16000, the highest average heat transfer coefficient $4855 W/m^2K$ was achieved.

Figure 4(b) presents heat transfer enhancement percentage of four different

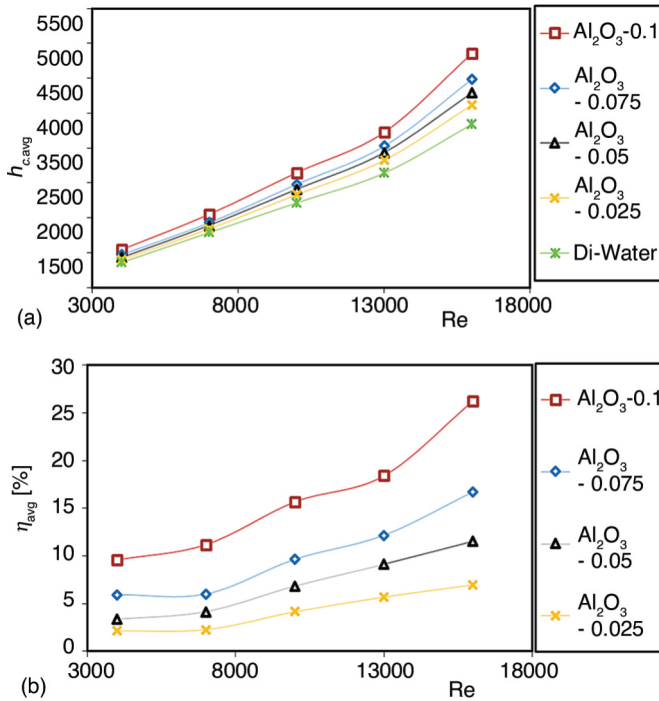


Figure 4. (a) Average heat transfer coefficient of Di-water and Al₂O₃-water nanofluids over a BFS and (b) average heat transfer coefficient enhancement vs. Reynolds number

weight concentrations (0.025, 0.05, 0.075, and 0.1 w.%) and five Reynolds numbers (4000, 7000, 10000, 13000, 16000) at a constant DC power supply of 600 W.

The average heat transfer coefficient increases with the increase of concentrations and Reynolds number. Results revealed that with the increase of Reynolds number from 4000 to 16000, the average (%) heat transfer coefficient enhancement (η) increased from 9.6 to 26.3% at weight concentration of 0.1% from 5.9 to 16.7% at weight concentration of 0.075 wt.% from 3.3 to 11.5% at weight concentration of 0.05 wt.%, and from 2.1 to 7% at weight concentration of 0.025 wt.%. Heat transfer enhancement in the presence of water-based Al₂O₃ nanofluid enhances linearly with the increase of concentration and Reynolds number.

Heat transfer enhancement with the increase of nanoparticles concentration in nanofluid has occurred due to the enhancement of the rate of energy exchange at laminar sub-layer as eddies formation increases with the increase of nanoparticles concentration. Kherbeet, *et al.*, [23] has reported that the enhancement of heat transfer is due to increase in energy exchange rates by random and irregular movements of particles as concentration increases. While, many researchers have reported that the heat transfer enhancement is due to the increase of thermal conductivity of fluid from the addition of nanoparticles to the fluid [3, 13, 14, 30-33]. In contrast Kherbeet, *et al.*, [23] reported that the heat transfer enhancement is due to increase in viscosity with an increase of nanoparticles concentration.

Viscosity gradient and a non-uniform shear rate source the particle migration which leads to higher heat transfer coefficient as numerically showed by some researchers [34]. On the other hand, Aravind, Baskar, Baby, Sabareesh, Das and Ramaprabhu [35] qualitatively studied and explained the cause of heat transfer enhancement which could be achieved by either decreasing thermal boundary layer thickness or increasing thermal conductivity.

Previously researchers have reported enhancement of heat transfer due to the increase of nanofluid concentration but still, the mechanism of heat transfer enhancement with the nanofluid concentration has not been clearly understood.

Figure 5 presents heat transfer coefficient (h_c) X/D over a range of Reynolds number for water and Al₂O₃-water based nanofluid at different weight concentration for the Reynolds number of 16000, 10000, and 4000. The results reveal that the maximum h_c increase with the increase of Reynolds number and concentration of nanoparticles in the fluid, which satisfies the findings of

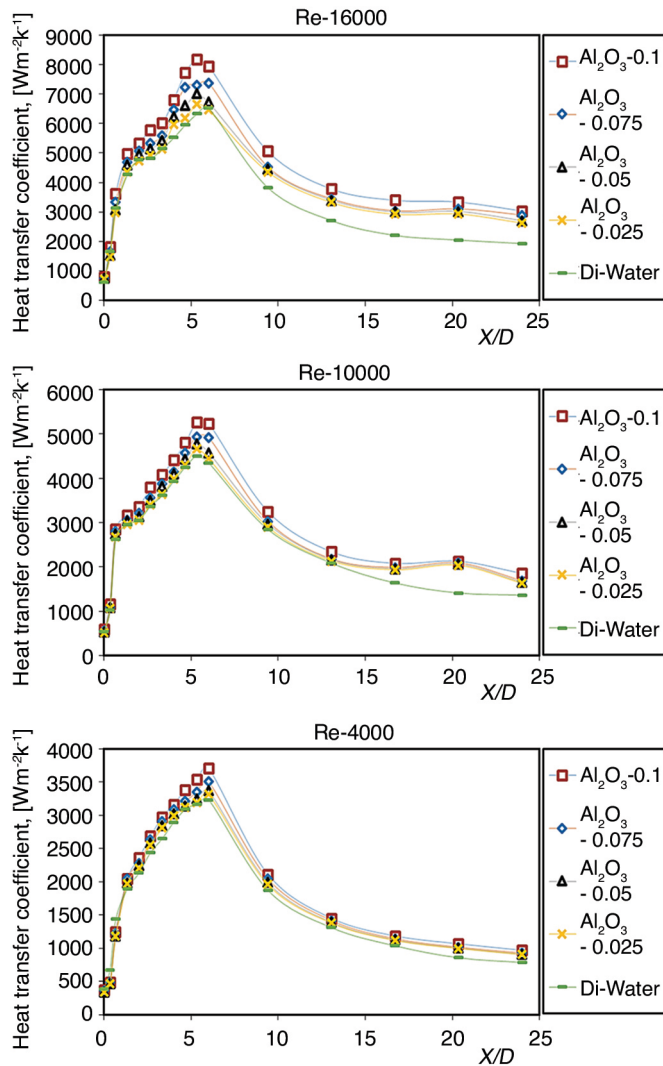


Figure 5. The effect of Reynolds numbers and weight concentrations of Al₂O₃-water nanofluids on the local heat transfer coefficient at different axial ratios

The figure also shows that the good PI curve is achieved at a weight concentration of 0.1 wt.% at different Reynolds numbers, followed by a gradual decrease of the PI with a decrease of Reynolds numbers and weight concentration.

Friction loss data in these experimental investigations are presented in the form of pressure drop as a function of Reynolds number. The data are presented in fig. 7 for water and Al₂O₃-water based nanofluids at four different concentrations (0.025, 0.05, 0.075 and 0.1 wt.%) at the Reynolds number range from 4000 to 16000.

Figure 7 shows the pressure drop enhances with the increase of Reynolds number and the highest pressure drop data point is observed at a higher weight concentration (0.1 wt.%) of Al₂O₃-water nanofluid and at the higher Reynolds number of 16000. Similarly, the lowest

other researchers [23]. The highest h_c were obtained at the higher Reynolds number of 16000 and weight concentration of 0.1 wt.%, similar results were obtained by the previous researcher for a study of heat transfer in BFS [36].

The PI (ϵ) that is the ratio of the heat transfer rate to the pressure drop, has been measured for the evaluation of the economic performance of the working fluids. Recently many researchers reported that the heat transfer performance improves with the addition of solid nanoparticles but along with heat transfer improvement it also sources additional undesirable pressure drop. Consequently, the PI is reported to assay both heat transfer and pressure drop. The deviations of the average PI for Al₂O₃-water nanofluids are presented at different weight concentrations and Reynolds numbers in fig. 6. It is observed that the PI of Al₂O₃-water nanofluid at all weight concentrations are higher than unity, that showing the effectiveness of the Al₂O₃-water nanofluids for being used over the BFS. Furthermore, it is observed that with the increase of weight concentration of solid alumina nanoparticles in nanofluids, the PI also increases as per expectation.

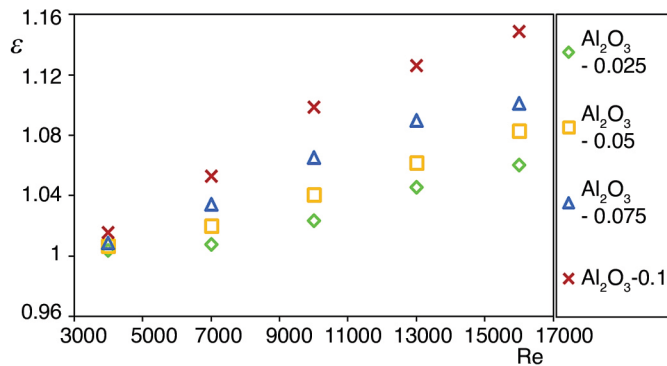


Figure 6. Performance index for the BFC in the presence of Di-water and Al₂O₃-water nanofluids with different weight concentration.

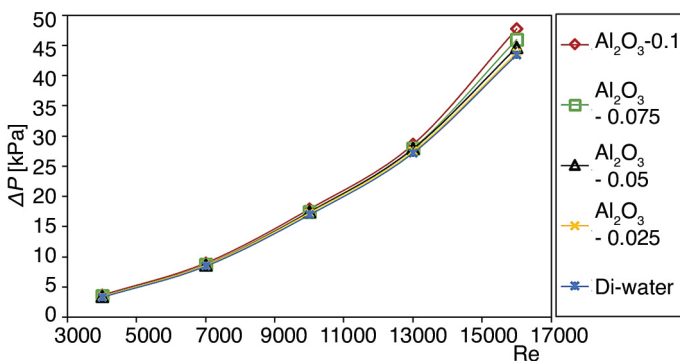


Figure 7. Experimental pressure drop of Di-water and Al₂O₃-water nanofluids at weight concentrations of 0.025 wt.%, 0.05 wt.%, 0.075 wt.%, and 0.1 wt.%, for different Reynolds number.

pressure peak is observed at the lower concentration (0.025 wt.%) of Al₂O₃-water nanofluid and at the lower Reynolds number of 4000. Although the difference in pressure drops are not significant in peaks of different concentrations of Al₂O₃-water nanofluids. The increase of pressure drop is due to increase of friction owing to increase of turbulence with the enhanced Reynolds number. Further, in fig.7 the addition of nanoparticles increases the viscosity of base fluid slightly due to which a little difference between the different curves at varying concentrations are observed. Contrary to the pressure drop of fiber suspensions studies, where with the increase of concentration and flow rate the pressure drop decreases [37].

Conclusions

The convective heat transfer of Al₂O₃-water nanofluid flowing in a horizontal backward-facing

step has experimentally investigated. Experiments have carried out for various concentrations and under turbulent flow conditions. The effects of concentrations and Reynolds number on the local heat transfer coefficient, average heat transfer coefficient, local Nusselt number, performance index, and pressure losses have systematically been investigated. It is concluded that the prepared Al₂O₃-water based nanofluids at a low concentration have a higher rate of heat transfer than that of Di-water. Heat transfer rate rises highly, at a loading of only 0.1 wt.% Al₂O₃ nanoparticles in Di-water, representing more than 26.3% enhancement. Also, heat transfer coefficient and Nusselt number of Al₂O₃-water nanofluids and Di-water for turbulent flow regime were measured experimentally for the first time over a backward-facing step. Furthermore, an increase of Reynolds number and the concentration of nanoparticles led to an increase of heat transfer rate. In addition, the pressure drop variation increases with the increase of Reynolds number and nanoparticles concentration but the changes are insignificant in the present range of investigation.

Acknowledgement

This research has been financially supported by, University of Malaya Research fund assistance BK063-2016, Research University Grant RF014A-2018, UMRG RP039C-15AET Faculty of Engineering, University of Malaya.

References

- [1] Mohammed, H., A. *et al.*, Influence of Nanofluids on Mixed Convective Heat Transfer Over a Horizontal Backward-Facing Step, *Heat Transfer-Asian Research*, 40 (2011), 4, pp. 287-307
- [2] Abu-Mulaweh, H., A Review of Research on Laminar Mixed Convection Flow Over Backward-and Forward Facing Steps, *International Journal of Thermal Sciences*, 42 (2003), 9, pp. 897-909
- [3] Masuda, H., *et al.*, Alteration of Thermal Conductivity and Viscosity of Liquid by Dispersing Ultra-Fine Particles. Dispersion of Al₂O₃, SiO₂, and TiO₂ Ultra-Fine Particles, *Netsu Bussei*, 7 (1993), 4, pp. 227-233
- [4] Koblinski, P., *et al.*, Mechanisms of Heat Flow in Suspensions of Nano-Sized Particles (nanofluids), *International Journal of Heat and Mass Transfer*, 45 (2002), 4, pp. 855-863
- [5] Xie, H.-Q., *et al.*, Thermal Conductivity of Suspensions Containing Nanosized SiC Particles, *International Journal of Thermophysics*, 23 (2002), 2, pp. 571-580
- [6] Wang, B.-X., *et al.*, A Fractal Model for Predicting the Effective Thermal Conductivity of Liquid with Suspension of Nanoparticles, *International Journal of Heat and Mass Transfer*, 46 (2003), 14, pp. 2665-2672
- [7] Ozerinc, S., *et al.*, Enhanced Thermal Conductivity of Nanofluids: A State-of-the-Art Review, *Microfluidics and Nanofluidics*, 8 (2010), 2, pp. 145-170
- [8] Beck, M. P., *et al.*, The Effect of Particle Size on the Thermal Conductivity of Alumina Nanofluids, *Journal of Nanoparticle Research*, 11 (2009), 5, pp. 1129-1136
- [9] Murugesan, C., S. Sivan, Limits for Thermal Conductivity of Nanofluids, *Thermal Science*, 14 (2010), 1, pp. 65-71
- [10] Chen, H., *et al.*, Predicting Thermal Conductivity of Liquid Suspensions of Nanoparticles (Nanofluids) Based on Rheology, *Particuology*, 7 (2009), 2, pp. 151-157
- [11] Solangi, K., *et al.*, A Comprehensive Review of Thermo-Physical Properties and Convective Heat Transfer to Nanofluids, *Energy*, 89 (2015), Sept., pp. 1065-1086
- [12] Mohammed, H., *et al.*, Convective Heat Transfer and Fluid Flow Study Over a Step Using Nanofluids: A Review, *Renewable and Sustainable Energy Reviews*, 15 (2011), 6, pp. 2921-2939
- [13] Sadri, R., K. *et al.*, Experimental Study on Thermo-Physical and Rheological Properties of Stable and Green Reduced Graphene Oxide nanofluids: Hydrothermal Assisted Technique, *Journal of Dispersion Science and Technology*, 38 (2017), 9, pp. 1302-1310
- [14] Hosseini, M., *et al.*, Experimental Study on Heat Transfer and Thermo-Physical Properties of Covalently Functionalized Carbon Nanotubes Nanofluids in an Annular Heat Exchanger: A Green and Novel Synthesis, *Energy & Fuels*, 31 (2017), 5, pp. 5635-5644
- [15] Boelter, L., *et al.*, An Investigation of Aircraft Heaters XXVII: Distribution of Heat-Transfer Rate in the Entrance Section of a Circular Tube, Report NACA-TN1451, NACA Technical Note, NACA, Washington DC, 1948
- [16] Ede, A., *et al.*, Effect on the Local Heat-Transfer Coefficient in a Pipe of an Abrupt Disturbance of the Fluid Flow: Abrupt Convergence and Divergence of Diameter Ratio 2/1, *Proceedings of the Institution of Mechanical Engineers*, 170 (1956), 1, pp. 1113-1130
- [17] Seban, R., Heat Transfer to Separated and Reattached Subsonic Turbulent Flows Obtained Downstream of a Surface Step, *Journal of the Aerospace Sciences*, 26 (2012), 12, pp. 809-814
- [18] Abbott, D., Experimental Investigation of Subsonic Turbulent Flow Over Single and Double Backward Facing Steps, *Journal of Basic Engineering*, 84 (1962), 3, pp. 317-325
- [19] Filetti, E., Kays W.M., Heat Transfer in Separated, Reattached, and Redevelopment Regions Behind a Double Step at Entrance to a Flat Duct, *Journal of Heat Transfer*, 89 (1967), 2, pp. 163-167
- [20] Goldstein, R. J., *et al.*, Laminar Separation, Reattachment, and Transition of the Flow Over a Downstream Facing Step, *Journal of Basic Engineering*, 92 (1970), 4, pp. 732-739
- [21] Abu-Nada, E., Application of Nanofluids for Heat Transfer Enhancement of Separated Flows Encountered in a Backward Facing Step, *International Journal of Heat and Fluid Flow*, 29 (2008), 1, pp. 242-249
- [22] Al-Aswadi, A. A., *et al.*, Laminar Forced Convection Flow Over a Backward Facing Step Using Nanofluids, *International Communications in Heat and Mass Transfer*, 37 (2010), 8, pp. 950-957
- [23] Kherbeet, A. S., *et al.*, The Effect of Nanofluids Flow on Mixed Convection Heat Transfer Over Microscale Backward-Facing Step, *International Journal of Heat and Mass Transfer*, 55 (2012), 21-22, pp. 5870-5881
- [24] Kherbeet, A. S., *et al.*, Combined Convection Nanofluid Flow and Heat Transfer Over Microscale Forward Facing Step, *International Journal of Nanoparticles*, 7 (2014), 1, pp. 1-25
- [25] Kherbeet, A. S., *et al.*, The Effect of Step Height of Microscale Backward-Facing Step on Mixed Convection Nanofluid Flow and Heat Transfer Characteristics, *International Journal of Heat and Mass Transfer*, 68 (2014), Jan., pp. 554-566

- [26] Kherbeet, A. S., *et al.*, Experimental Study of Nanofluid Flow and Heat Transfer Over Microscale Backward- and Forward-Facing Steps, *Experimental Thermal and Fluid Science*, 65 (2015), July, pp. 13-21
- [27] Yu, W., *et al.*, Heat Transfer to a Silicon Carbide/Water Nanofluid, *International Journal of Heat and Mass Transfer* 52 (2009), 15-16, pp. 3606-3612
- [28] Yu, W., *et al.*, Comparative Review of Turbulent Heat Transfer of Nanofluids, *International Journal of Heat and Mass Transfer* 55 (2012), 21-22, pp. 5380-5396
- [29] Ahmed, S. M., *et al.*, Effect of Various Refining Processes for Kenaf Bast Non-Wood Pulp Fibers Suspensions on Heat Transfer Coefficient in Circular Pipe Heat Exchanger, *Heat and Mass Transfer*, 54 (2017), 3, pp. 875-882
- [30] Choi, S., *et al.*, Anomalous Thermal Conductivity Enhancement in Nanotube Suspensions, *Applied physics letters*, 79 (2001), 14, pp. 2252-2254
- [31] Lee, S., *et al.*, Measuring Thermal Conductivity of Fluids Containing Oxide Nanoparticles, *Journal of Heat transfer*, 121 (1999), 2, pp. 280-289
- [32] Amiri, A., *et al.*, Functionalization and Exfoliation of Graphite Into Mono Layer Graphene for Improved Heat Dissipation, *Journal of the Taiwan Institute of Chemical Engineers*, 71 (2017), Feb, pp. 480-493
- [33] Sadri, R., *et al.*, A Novel, Eco-Friendly Technique for Covalent Functionalization of Graphene Nanoplatelets and the Potential of Their Nanofluids for Heat Transfer Applications, *Chemical Physics Letters*, 675 (2017), May, pp. 92-97
- [34] Wen, D., Ding, Y., Effect of Particle Migration on Heat Transfer in Suspensions of Nanoparticles Flowing Through Minichannels, *Microfluidics and Nanofluidics*, 1 (2005), 2, pp. 183-189
- [35] Aravind, S. J., *et al.*, Investigation of Structural Stability, Dispersion, Viscosity, and Conductive Heat Transfer Properties of Functionalized Carbon Nanotube Based Nanofluids, *The Journal of Physical Chemistry C* 115 (2011), 34, pp. 16737-16744
- [36] Amiri, A., *et al.*, Backward-Facing Step Heat Transfer of the Turbulent Regime for Functionalized Graphene Nanoplatelets Based Water–Ethylene Glycol Nanofluids, *International Journal of Heat and Mass Transfer*, 97 (2016) June, pp. 538-546
- [37] Ahmed, S. M., *et al.*, Experimental Investigation on Momentum and Drag Reduction of Malaysian Crop Suspensions in Closed Conduit Flow, *IOP Conference Series: Materials Science and Engineering*, 210 (2017), 1, 012065